ISSN 1063-780X, Plasma Physics Reports, 2023, Vol. 49, No. 11, pp. 1350–1357. © The Author(s), 2023. This article is an open access publication.
Russian Text © The Author(s), 2023, published in Fizika Plazmy, 2023, Vol. 49, No. 11, pp. 1170–1177.

LOW-TEMPERATURE PLASMA

Kinetic Model of Vacuum Plasma Expansion in a Cylindrical Gap

V. Yu. Kozhevnikov[a], A. V. Kozyrev[a,*], A. O. Kokovin[a], and N. S. Semenyuk[a]

[a] *Institute of High Current Electronics, Siberian Branch, Russian Academy of Sciences, Tomsk, 634055 Russia*

**e-mail: kozyrev@to.hcei.tsc.ru*

Received May 21, 2023; revised August 28, 2023; accepted September 1, 2023

Abstract—Results of a theoretical description of collisionless kinetics of radial expansion of two-component (electron–ion) plasma in the one-dimensional cylindrical formulation of the problem are presented. The electric-field mechanism of supersonic expansion of the plasma flame due to the motion of the electron–ion ensemble and self-consistent electric field in the diode with the potential difference applied to it is demonstrated. The spatiotemporal evolution of the ion energy distribution function, electric potential, and rate of expansion of the emission boundary of the plasma flame is shown. The calculated rates of flame expansion at the copper cathode (~1.5×10^6 cm/s) well agree with the experimental data.

Keywords: kinetics of rarefied plasma, collisionless plasma, cathode flame, vacuum discharge

DOI: 10.1134/S1063780X23601256

INTRODUCTION

Vacuum gap breakdown is widely studied and used in technical equipment with unique characteristics [1, 2]. Vacuum breakdown is excited by plasma due to explosions of microscopic irregularities of the cathode, which is followed by expansion of the cathode flame plasma into the interelectrode gap. One of key problems of vacuum electronics is the process of expansion of initiated near-cathode plasma. This process is characterized by superthermal expansion rates and anomalous ion transfer to the anode in the vacuum discharge [3–5]. The plasma expansion rate recorded in vacuum discharges with different cathode materials amounts to $(1–4) \times 10^6$ cm/s [6], which corresponds to the ion kinetic energy of tens and, sometimes, hundreds of electron-volts [7–9]. The energies of ions arriving at the anode can exceed the arcing voltage (multiplied by the elementary charge) of the arc discharge stage which is formed as a result of plasma bridging of the gap. Due to this property, fast anode-directed ion fluxes are sometimes called anomalous.

The nature and the formation mechanism of such fluxes still have no commonly accepted explanation and are a subject of numerous and long-term discussions among specialists on vacuum discharge. The discussions take place mainly within the framework of three noticeably distinguishing approaches to explaining anode-directed ion fluxes: (1) the hydrodynamic model of plasma acceleration due to the high pressure gradient of the substance outflowing from the micrometer-size explosive emission center [10, 11]; (2) the electron wind model which explains the ion acceleration by collisions with a very dense electron flux which, again, takes place in the region of the compact explosive emission center [12, 13]; and (3) the model of field acceleration of ions due to the nonmonotonic electric potential distribution ("potential hump") which can take place in a close neighborhood of the explosive emission center [14, 15]. In all these models, the key role is played by the compact explosive emission center the traces of which are associated with micrometer craters on the surface of the vacuum discharge cathode.

Not questioning the possibility of implementing the three abovementioned mechanisms, we call plasma physics specialists' attention to the possibility in principle for another (electric-field) fundamental mechanism of collisionless plasma expansion in the vacuum gap to which electric voltage is applied. Here, the term "fundamental" is used in its literal sense as "the most general and/or simple," i.e., not fraught by physical complexity of the process of initiating the explosive emission center and formation of the atom–ion composition of the plasma.

Here, we formulate an ultimately simplified physico-mathematical problem (the plasma is assumed to be consisting of two components and collisionless, and the motion is assumed to be one-dimensional) and solve it in terms of physical kinetics. Certainly, plane geometry would be a simpler one-dimensional problem; however, the radially diverging plasma expansion, without complicating the mathematical equations, makes it possible to additionally study the influence of the degree of spatial inhomogeneity of the problem on characteristics of the process.

MATHEMATICAL MODEL OF THE EXPANSION

The evolution of two-component plasma consisting of electrons and singly charged ions in a vacuum cylindrical gap is described by two Vlasov equations which take into account the centrifugal forces F_e and F_i caused by the initial spread of azimuthal momentums of particles:

$$\frac{\partial f}{\partial t} + \frac{p}{m}\frac{1}{r}\frac{\partial}{\partial r}(rf) + \frac{\partial}{\partial p}\left[(-qE + F_e)f\right] = 0, \quad (1)$$

$$\frac{\partial F}{\partial t} + \frac{p}{M}\frac{1}{r}\frac{\partial}{\partial r}(rF) + \frac{\partial}{\partial p}\left[(qE + F_i)F\right] = 0, \quad (2)$$

where $f(r, p, t)$ and $F(r, p, t)$ are the distribution functions of electrons and ions with respect to coordinates r and radial momentums p; m and M are the masses of the electron and ion, respectively; q is the elementary charge; and $E(r,t)$ is the electric field strength.

The additional term $F_{e,i} = p_\varphi^2/mr$ in Eqs. (1) and (2) takes into account the action of centrifugal forces in the presence of the transverse (azimuthal) momentum in the particles. Although we solve the problem of radial expansion of plasma in a vacuum gap, the ensemble of particles of the initiating plasma can contain nonzero angular momentums which are preserved in the process of radial expansion of particle ensembles and have an effect on the dynamics of the electric field. These momentums p_φ^2 can be immediately averaged using the law of conservation of the azimuthal momentum $r_C p_{\varphi C} = r p_\varphi$:

$$\left\langle p_\varphi^2 \right\rangle = \frac{r_C^2}{r^2}\left\langle p_{\varphi C}^2 \right\rangle = \frac{r_C^2}{r^2}\int_{-\infty}^{\infty} p_{\varphi C}^2 f_{\varphi C} dp_\varphi,$$
$$f_{\varphi C} = \frac{1}{\sqrt{2\pi m T}}\exp\left(-\frac{p_{\varphi C}^2}{2mT}\right), \quad (3)$$

where r_C is the plasma cathode radius (the parameter of the problem); $p_{\varphi C}$ is the angular component of the particle momentum at the cathode; $f_{\varphi C}$ is the Maxwellian distribution function of azimuthal momentums at the cathode; and T is the thermodynamic temperature of the cathode ensemble. As a result, the centrifugal forces for electrons and ions have the form

$$F_e = \frac{T_e r_C^2}{r^3}, \quad F_i = \frac{T_i r_C^2}{r^3}. \quad (4)$$

We added the azimuthal momentums into the calculated model because they create the centrifugal pseudoforce of inertia which can have a significant effect on the transfer of the particle flux in regions filled with quasineutral plasma, where the electric field strength is close to zero values.

Equations (1) and (2) are complemented by the Poisson equation

$$\frac{1}{r}\frac{\partial}{\partial r}\left(r\frac{\partial \varphi}{\partial r}\right) = -\frac{\rho}{\varepsilon_0} = -\frac{q(n_i - n_e)}{\varepsilon_0}, \quad (5)$$

where $\varphi(r,t)$ is the electric potential; $\rho(r,t)$ is the volume charge density; ε_0 is the electric constant; and $n_e(r,t)$ and $n_i(r,t)$ are the electron and ion densities which are determined as moments of the distribution functions

$$n_e = \int_0^\infty f dp, \quad n_i = \int_0^\infty F dp. \quad (6)$$

The Poisson equation with allowance for the boundary conditions at the cathode r_C and anode r_A: $\varphi(r_C, t) = 0$ and $\varphi(r_A, t) = U(t)$—has an exact solution in quadratures

$$\varphi = \left[U + \int_{r_C}^{r_A}\frac{1}{r''}\left\{\int_{r_C}^{r''} r'\frac{\rho}{\varepsilon_0}dr'\right\}dr''\right]\frac{\ln r/r_C}{\ln r_A/r_C} - \int_{r_C}^{r}\frac{1}{r''}\left\{\int_{r_C}^{r''} r'\frac{\rho}{\varepsilon_0}dr'\right\}dr''. \quad (7)$$

The electric field strength

$$E = -\frac{\partial \varphi}{\partial r} = -\left[U + \int_{r_C}^{r_A}\frac{1}{r''}\left\{\int_{r_C}^{r''} r'\frac{\rho}{\varepsilon_0}dr'\right\}dr''\right] \times \frac{1}{r\ln r_A/r_C} + \frac{1}{r}\left\{\int_{r_C}^{r} r'\frac{\rho}{\varepsilon_0}dr'\right\}. \quad (8)$$

Further, we suppose that the series electrical circuit consists of a voltage source $U_{\text{source}}(t)$, a ballast resistance R_{ballast}, and a discharge gap. Then, the voltage at the electrodes U is described by the circuit equation

$$U = U_{\text{source}} - j_{\text{total}} R_{\text{ballast}} S, \quad (9)$$

where $S(r) = 2\pi r L$ is the area of the current cylindrical surface and L is the axial extension of the discharge. The total current density $j_{\text{total}}(r,t)$ includes the displacement current density and the convective densities of the electron and ion currents $j_e(r,t)$ and $j_i(r,t)$:

$$j_{\text{total}} = \varepsilon_0\frac{\partial E}{\partial t} + j_e + j_i. \quad (10)$$

The convective current densities are determined in terms of the distribution function moments

$$j_e(r,t) = -q\int_{-\infty}^{\infty}\frac{p}{m}f dp, \quad j_i(r,t) = q\int_{-\infty}^{\infty}\frac{p}{M}F dp. \quad (11)$$

Let us average Eq. (10) over the gap radius and obtain the equation for the total current

$$j_{\text{total}}(t) = -\frac{\varepsilon_0}{r_A - r_C}\frac{dU}{dt} + J(t),$$
$$J(t) = \frac{1}{r_A - r_C}\int_{r_C}^{r_A}(j_e + j_i)dr. \quad (12)$$

Substituting the voltage U from (9) into (12), we obtain the equation for the discharge current

$$\frac{dj_{\text{total}}}{dt} = \frac{1}{\tau_R}\left(j_{\text{total}}(t) + \frac{\varepsilon_0}{r_A - r_C}\frac{dU_{\text{source}}}{dt} - J(t)\right),$$
$$\tau_R = \frac{\varepsilon_0 R_{\text{ballast}} S}{r_A - r_C}. \quad (13)$$

Integrating (13), we obtain an explicit expression for the current density in the discharge gap

$$j_{\text{total}} = \frac{e^{t/\tau_R}}{\tau_R}\int_0^t\left[\frac{\varepsilon_0}{r_A - r_C}\frac{dU_{\text{source}}}{dt} - J(t')\right]e^{-t'/\tau_R}dt'. \quad (14)$$

Finally, the mathematical model of the discharge should be complemented by specifying the function of the external voltage source $U_{\text{source}}(t)$ and boundary conditions at the cathode.

We assume that the cathode surface is a nonequilibrium electron–ion quasineutral plasma with a given density n_0 the ensembles of which are characterized by Maxwellian distributions with different thermodynamic temperatures T_e, T_i and a nonzero average momentum:

$$f_0 dp = n_0\frac{1}{\sqrt{2\pi m T_e}}\exp\left(-\frac{(p - \sqrt{mT_e})^2}{2mT_e}\right)dp,$$
$$F_0 dp = n_0\frac{1}{\sqrt{2\pi M T_i}}\exp\left(-\frac{(p - \sqrt{MT_i})^2}{2MT_i}\right)dp. \quad (15)$$

The initial distribution functions (15) were given with a displaced momentum to avoid the artificial gap in the particle flux at the boundary of the computational domain (at $r = r_C$, it would be zero by definition for an unbiased distribution) and in the radial flux outside this boundary (at $r > r_C$). This trick generates smooth solutions in a neighborhood of the cathode boundary ($r = r_C + 0$).

The system of five equations (1), (2), (8), (9), and (14), jointly with boundary conditions (15), forms a closed mathematical model of a one-dimensional vacuum diode with plasma emission of particles at the cathode. This system of equations is solved numerically by semi-Lagrangian methods. For the calculated phase space (r, t), a nonuniform grid with dimensions of 4000 × 5000 elements is used for discretization of each of Eqs. (1) and (2).

PLASMA EXPANSION IN A CYLINDRICAL GAP

The calculations show that the expansion mechanism remains almost unchanged under reasonable variations of the initial parameters ($r_C = 20$–1000 μm, $U_{\text{source}} = 100$–2000 V, and $n_0 = 10^{12}$–10^{16} cm^{-3}); for this reason, we present quantitative results only for a certain typical case. The choice of the applied voltage U_{source} and ballast resistance R_{ballast} was usually caused by the condition that the circuital current provided a noticeable decrease in the anode voltage as the plasma approached the anode radius.

Below, we present the calculations of plasma dynamics in a cylindrical vacuum gap with the cathode radius $r_C = 1$ mm, anode radius $r_A = 10$ mm, and longitudinal length $L = 10$ mm. The voltage source generates a pulse $U_{\text{source}}(t)$ with an amplitude of 2 kV and short rise time $t_{\text{rise}} = 0.1$ ns; it is connected to the gap through a ballast resistance $R_{\text{ballast}} = 100\ \Omega$. At the cathode radius, the state of quasineutral plasma with density $n_0 = 10^{14}$ cm^{-3} of electrons and single-charged copper ions Cu^+ was recorded. This density provides by wide margins the collisionless regime of charged particle motion in a centimeter gap. The electron and ion temperatures are $T_e = 3$ eV and $T_i = 1$ eV. At these parameters, the density of the thermal current of electron emission (~464 A/cm^2) exceeds by orders of magnitudes the density of the Child–Langmuir current

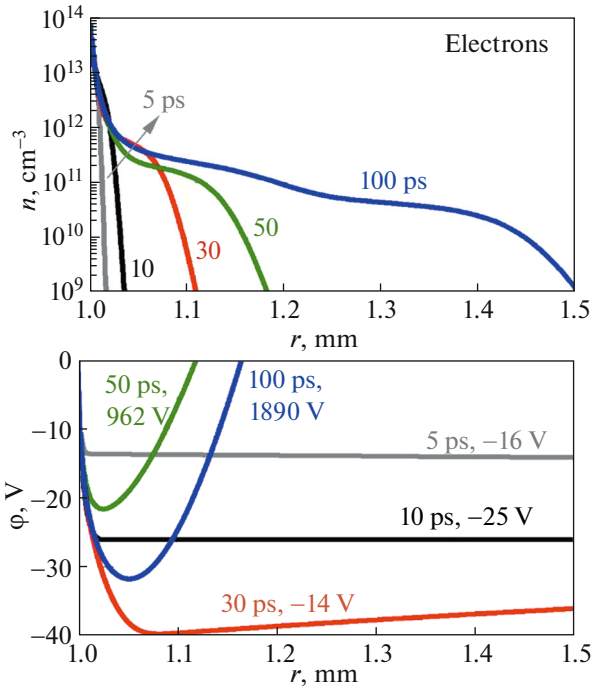

Fig. 1. Electron density n and distribution of the electric potential φ near the cathode at first time instants (the anode voltages are shown near the time).

$j_{CL} \approx (4\varepsilon_0/9)\sqrt{2q/m}(U^{3/2}/r_C r_A)$ [16] at the cathode of a cylindrical diode (~2 A/cm^2) operating in the regime of current limitation by the spatial charge of electrons.

Initial Stage of Expansion—Formation of a Virtual Cathode

In the first picoseconds, when the voltage at the source is still low, electrons already move towards the anode. In this process, they generate current in the circuit and form a region of a negative potential (of a virtual cathode). This negative potential reflects the major part of cathode plasma electrons and transmits to the anode only a small amount of them. The potential well depth after 30 ps reaches –40 V, and it also changes with a change in the applied anode voltage. The dynamics of this process in time is shown in Fig. 1. This starting stage of the electron motion is essential for understanding the electric-field mechanism of plasma expansion. For this reason, we so comprehensively demonstrate the distribution of the electron cloud and electric potential until the ions remain almost immobile at the boundary of the cathode plasma. Note that first electrons reach the anode only by the time instant of 480 ps.

We immediately note that we counted up the starting stage of the expansion under different initial conditions. For example, the plasma density could be smoothly triggered from zero $n_0(t)$ or be exponentially spread in the space: $f_0(r_C + x, v) = f_0(v)\exp(-x^2/l^2)$. Test calculations of this stage were also carried out by the large-particle method (PIC). All these tricks did not change qualitatively the abovementioned picture of the virtual cathode formation.

Extension of the Emission Boundary of Quasineutral Plasma

The negative potential of the virtual cathode near the plasma boundary is accelerating for ions. Therefore, the ions begin the natural motion to the anode; on this way, they compensate the spatial charge of the electron cloud and form the outer emission boundary of the cathode flame, as is shown in Fig. 2. By the emission plasma boundary we mean the cross section

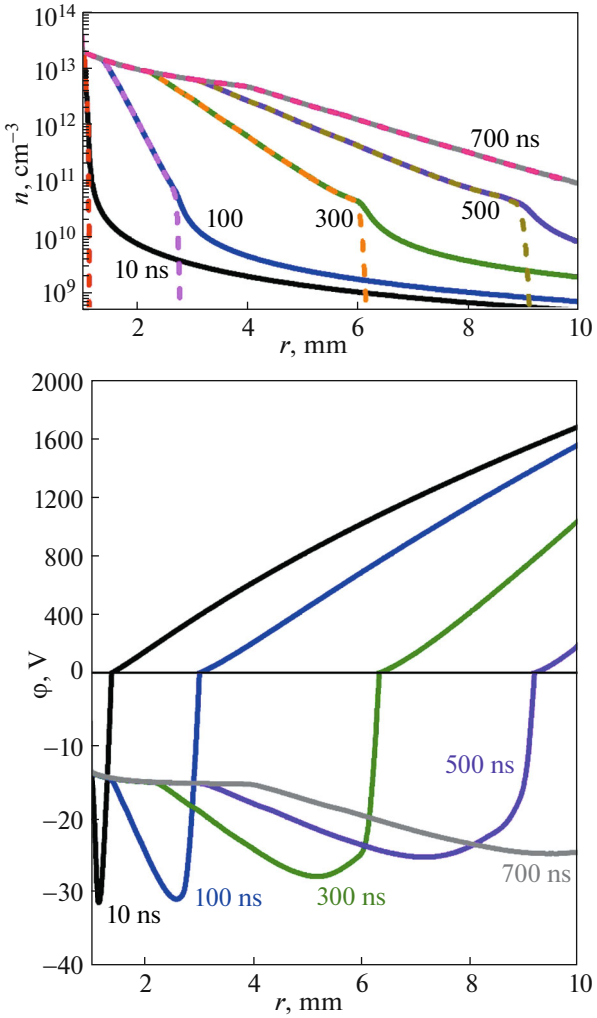

Fig. 2. Distribution of the particle density (the solid line is electrons; the dashed line, ions) and electric potential distribution (here, the scales of negative and positive values are different).

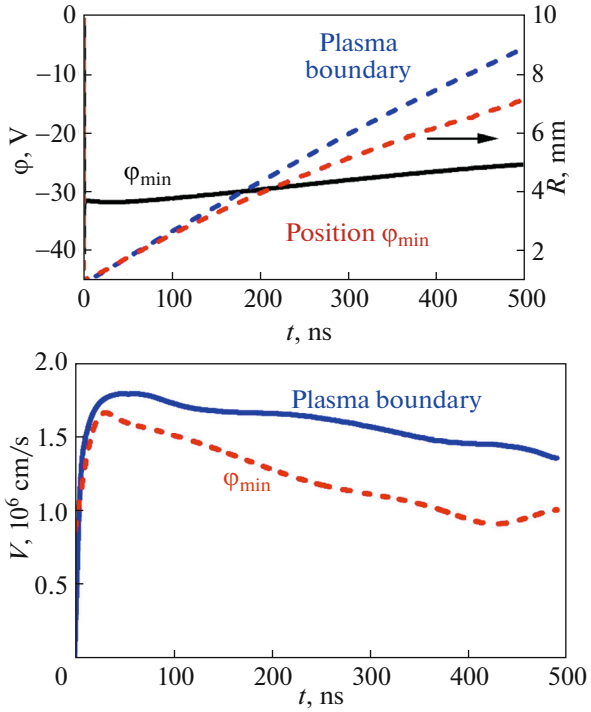

Fig. 3. Time dependences of the position and depth of the potential well and emission plasma boundary (top). Motion speeds of the plasma boundary and point of minimum of the potential V (bottom).

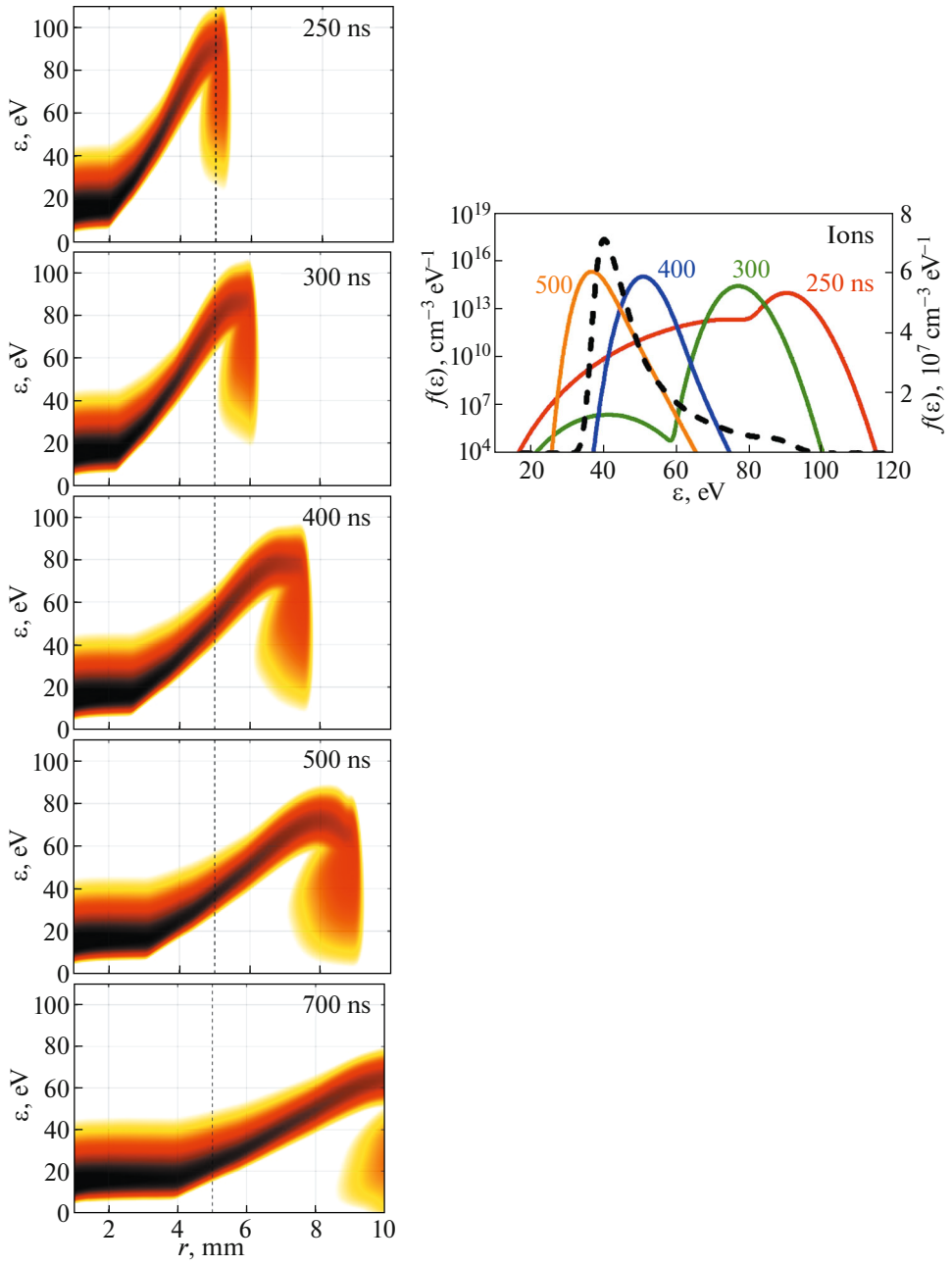

Fig. 4. Phase portraits of the ion energy distribution function $f(\varepsilon)$ at different time instants (on the left) and instantaneous ion spectra of $f(\varepsilon)$ in the radial cross section marked by the dashed line (on the right).

where the electron and ion densities begin to noticeably diverge (in Fig. 2, this divergence is visible when $\Delta n/n_0 \sim 20\%$). The ions gain energy in the accelerating field and move to the anode; in this process, they displace both the boundary of quasineutral plasma and the cross section of the virtual cathode to the anode.

As the emission boundary of the flame moves to the anode, the current in the electric circuit increases, which leads to a decrease in the voltage at the anode, as it follows from (9). We call attention to the fact that the plasma density in the neighborhood of the emission boundary remains approximately at the same level of ~6×10^{10} cm^{-3}, which is lower than the cathode plasma density by three orders of magnitude.

Figure 3 shows the position and motion velocity of the cross section of the virtual cathode and emission plasma boundary as functions of time. It is seen that the emission boundary gradually detaches from the cross section of the minimum potential (of the virtual cathode), and they move with different velocities. The

motion of the virtual cathode provides ion acceleration to the anode. As a result, the average energy of ions in the gap reaches tens of electron-volts, which considerably exceeds their thermal energy in cathode plasma (~1 eV).

Energy Spectra of Ions in Expanding Plasma

Figure 4 presents the ion distribution functions in the phase plane (radius–energy) at different time instants and instantaneous spectra in the cross section $r = 5$ mm (this cross section corresponds to the dashed line in the phase portraits). The decrease in the ion energy in the right branch of the phase portrait is caused by reflection of the ion flux from the anode potential barrier. Let us pay attention to the fact that the anode potential decreases as the plasma approaches the anode (it is seen in the right Fig. 2); it can become close to zero and even negative, which provides physical arrival of ions at the anode.

To correctly estimate the width of instantaneous spectral distributions, we call attention to the logarithmic scale of the ordinate axis. The same figure shows the total spectrum of ions in the middle part of the gap; its maximum is in correspondence with energy of 40 eV (here, the scale of the ordinate axis is linear), and the width at half maximum is approximately equal to 15 eV. This indicates not only the formation of a directed flux of fast ions but also a high average thermal straggling of the velocities. In fact, this is about a very hot flux of matter.

VARIATION OF THE CATHODE RADIUS AND APPLIED VOLTAGE

To study the influence of the initial parameters of the problem on the process of plasma expansion, we performed comparative calculations with variation of the cathode radius. In doing this, other parameters (the applied voltage, resistance of the circuit, and cathode plasma density) remained unchanged. A change in the cathode radius at an unchanged density will lead to a change in the Child–Langmuir current density at the cathode. For the cathode radius of 0.05, 0.1, 0.5, and 1.0 mm, the Child–Langmuir current density takes values of 41.7, 20.8, 4.2, and 2.1 A/cm^2, respectively. However, in all the cases, the emission current density (464 A/cm^2) exceeds the Child–Langmuir current density more than by an order of magnitude.

The mechanism of plasma expansion in the gap does not change qualitatively with a change in the cathode radius. However, the potential well depth and, as a consequence, the advance speed of plasma to the anode change, as is shown in Fig. 5.

A similar situation of preservation of the expansion mechanism also takes place when varying the applied voltage, which is demonstrated by Fig. 6. For example, with a decrease in the applied potential, the potential well depth increases and plasma expands noticeably faster.

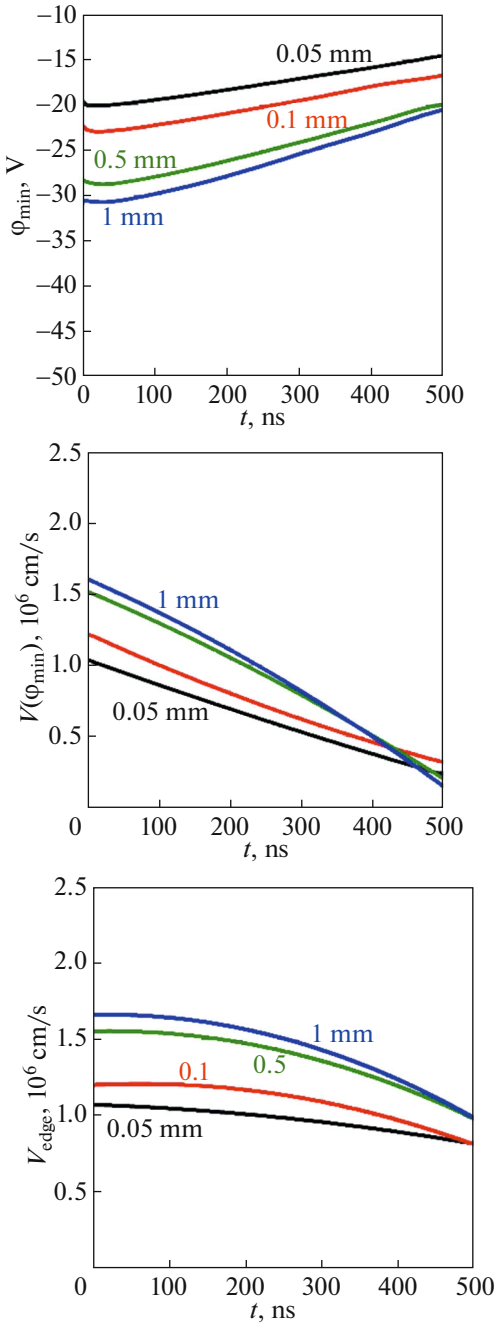

Fig. 5. Potential well φ_{min}, its velocity $V(\varphi_{min})$, and velocity of the emission plasma boundary V_{edge} at different time instants for cathodes with radii of 0.05, 0.1, 0.5, and 1.0 mm at the applied voltage of 2.0 kV.

Thus, variation of two key parameters of the problem leads to a noticeable quantitative variation in characteristics of the process of plasma expansion; however, the physical mechanism itself remains qualita-

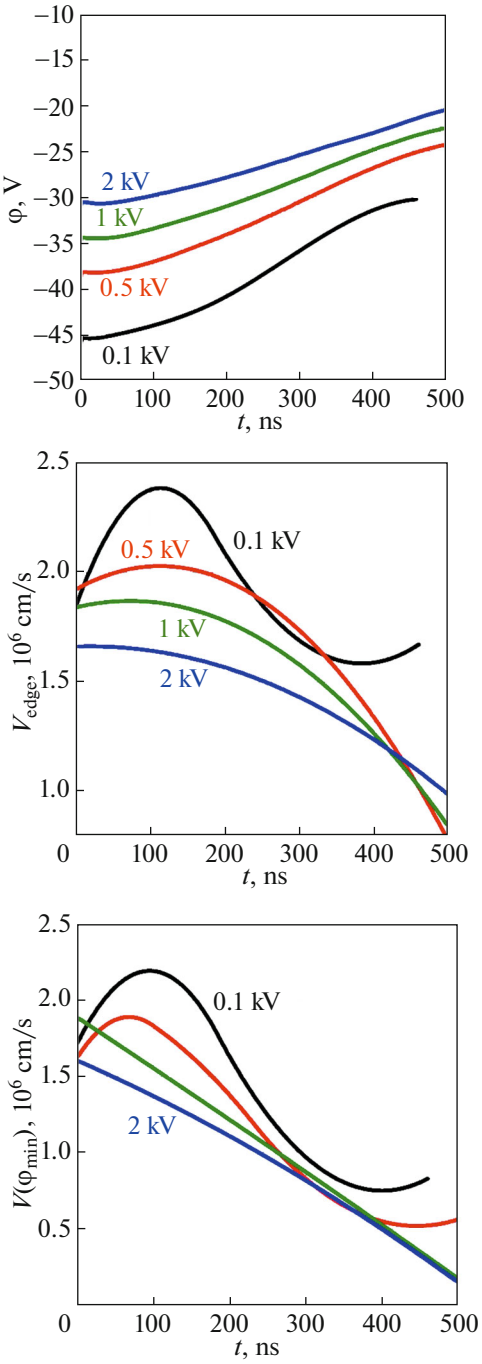

Fig. 6. Potential well, its velocity, and velocity of the emission plasma boundary at different time instants for a cathode with a radius of 1 mm and applied potential of 0.1, 0.5, 1.0, and 2.0 kV.

tively the same, which indicates its fundamental reliability.

CONCLUSIONS

The physical kinetics method allows one to mathematically correctly (in the form of smooth functions without breaks of continuity) describe the behavior of expanding longitudinally inhomogeneous plasma from the surface of which the electron emission current is taken off.

Within the framework of the kinetic calculation of the motion of the electron and ion components in a self-consistent electric field, the electric-field mechanism of cathode plasma expansion in a coaxial vacuum gap has been described in detail. The key factor having an effect on the dynamics of collisionless plasma is noted—this is the formation of a virtual cathode with a potential drop depth of tens of volts due to fast removal of electrons to the anode. The further motion of ions in the accelerating electric field leads to a fast advance of the plasma boundary and formation of a flux of ions with energies of tens of electron-volts.

The physical mechanism of plasma expansion presented here remains valid until the Child–Langmuir current density is significantly lower than the density of the thermal electron current in cathode plasma. If this relation is broken, the change of the mechanism of collisionless plasma expansion is highly probable. Its study will be a subject of further investigations. An evidence of this can be seen in Fig. 6, where the case of low voltage (100 V) noticeably falls out of the general trend.

Certainly, this heavily simplified model of plasma expansion cannot be directly applied to real vacuum arc discharges in which a significant role is played by locally inhomogeneous and nonstationary explosive emission processes, fast plasma jets, etc. However, abstracting from details of microturbulence on the surface of the vacuum arc cathode and treating the extended cathode of the arc as a source of dense and, on the average, homogeneous electron-emitting plasma, our calculations convincingly indicate the inevitable appearance of ion flux velocities observed experimentally [7, 8, 12].

FUNDING

This study was supported by the Russian Science Foundation, project no. 23-29-00239.

CONFLICT OF INTEREST

The authors of this work declare that they have no conflicts of interest.

OPEN ACCESS

This article is licensed under a Creative Commons Attribution 4.0 International License, which permits use, sharing, adaptation, distribution and reproduction in any medium or format, as long as you give appropriate credit to the original author(s) and the source, provide a link to the Creative Commons license, and indicate if changes were made. The images or other third party material in this article are included in the article's Creative Commons license, unless indicated other-

wise in a credit line to the material. If material is not included in the article's Creative Commons license and your intended use is not permitted by statutory regulation or exceeds the permitted use, you will need to obtain permission directly from the copyright holder. To view a copy of this license, visit http://creativecommons.org/licenses/by/4.0/.

REFERENCES

1. *Handbook of Vacuum Arc Science and Technology: Fundamentals and Applications,* Ed. by R. L. Boxman, D. M. Sanders, and P. J. Martin (Noyes, Park Ridge, NJ, 1995).
2. I. G. Brown, J. E. Galvin, and R. A. MacGill, Appl. Phys. Lett. **47**, 358 (1985).
3. A. Anders, *Cathodic Arcs: From Fractal Spots to Energetic Condensation* (Springer, New York, 2008).
4. I. I. Beilis, IEEE Trans. Plasma Sci. **29**, 657 (2001).
5. P. Chapelle, J. P. Bellot, H. Duval, A. Jardy, and D. Ablitzer, J. Phys. D: Appl. Phys. **35**, 137 (2001).
6. E. Hantzsche, IEEE Trans. Plasma Sci. **31**, 799 (2003).
7. W. D. Davis and H. C. Miller, J. Appl. Phys. **40**, 2212 (1969).
8. I. Brown and E. Oks, IEEE Trans. Plasma Sci. **33**, 1931 (2005).
9. A. Anders, Phys. Rev. E: Stat. Phys., Plasmas, Fluids, Relat. Interdiscip. Top. **55**, 969 (1997).
10. N. B. Volkov and A. Z. Nemirovsky, J. Phys. D: Appl. Phys. **24**, 693 (1991).
11. G. W. McClure, J. Appl. Phys. **45**, 2078 (1974).
12. G. Y. Yushkov, A. S. Bugaev, I. A. Krinberg, and E. M. Oks, Dokl. Phys **46**, 307 (2001).
13. S. A. Barengolts, G. A., Mesyats, and D. L. Shmelev, J. Exp. Theor. Phys. **93**, 1065 (2001).
14. A. A. Plyutto, V. N. Ryzhkov, and A. T. Kapin, Sov. Phys. JETP **20**, 328 (1965).
15. A. V. Bolotov, A. V. Kozyrev, and Yu. D. Korolev, Plasma Phys. Rep. **19**, 365 (1993).
16. V. L. Granovskii, *Electrical Current in Gas: Steady-State Current* (Nauka, Moscow, 1971) [in Russian].

Translated by A. Nikol'skii

Publisher's Note. Pleiades Publishing remains neutral with regard to jurisdictional claims in published maps and institutional affiliations.